ELSEVIER

Biochimica et Biophysica Acta 1567 (2002) 113–122

BIOCHIMICA ET BIOPHYSICA ACTA
BBA

www.bba-direct.com

Estimation of the radius of the pores formed by the *Bacillus thuringiensis* Cry1C δ-endotoxin in planar lipid bilayers

Olivier Peyronnet[a], Brian Nieman[a], Francis Généreux[a], Vincent Vachon[a], Raynald Laprade[a], Jean-Louis Schwartz[a,b,*]

[a] *Groupe de recherche en transport membranaire, Université de Montréal, P.O. Box 6128, Centre Ville Station, Montreal, Quebec, Canada H3C 3J7*
[b] *Biotechnology Research Institute, National Research Council, 6100 Royalmount Avenue, Montreal, Quebec, Canada H4P 2R2*

Received 26 June 2002; received in revised form 18 September 2002; accepted 19 September 2002

Abstract

Pore formation constitutes a key step in the mode of action of *Bacillus thuringiensis* δ-endotoxins and various activated Cry toxins have been shown to form ionic channels in receptor-free planar lipid bilayers at high concentrations. Multiple conductance levels have been observed with several toxins, suggesting that the channels result from the multimeric assembly of a variable number of toxin molecules. To test this possibility, the size of the channels formed by Cry1C was estimated with the non-electrolyte exclusion technique and polyethylene glycols of various molecular weights. In symmetrical 300 mM KCl solutions, Cry1C induced channel activity with 15 distinct conductance levels ranging from 21 to 246 pS and distributed in two main conductance populations. Both the smallest and largest conductance levels and the mean conductance values of both populations were systematically reduced in the presence of polyethylene glycols with hydrated radii of up to 1.05 nm, indicating that these solutes can penetrate the pores formed by the toxin. Larger polyethylene glycols had little effect on the conductance levels, indicating that they were excluded from the pores. Our results indicate that Cry1C forms clusters composed of a variable number of channels having a similar pore radius of between 1.0 and 1.3 nm and gating synchronously.

Keywords: Cry1C δ-endotoxin; Planar lipid bilayer; Ion channel; Polyethylene glycol; Pore size; *Bacillus thuringiensis*

1. Introduction

Cry δ-endotoxins are highly specific pore-forming toxins produced by the common Gram-positive bacterium *Bacillus thuringiensis* which has been widely used as an alternative to chemical insecticides for controlling forest and agricultural insect pests and vectors of human and animal diseases for several decades. Toxins of the Cry1 family are produced as 125–140 kDa crystalline protein precursors that are solubilized in the insect midgut and proteolytically converted into 55–75 kDa active proteins. The activated toxins interact with protein binding sites located on the apical membrane of midgut epithelial columnar cells and insert into the membrane to create ion-permeable pores. Formation of such pores disrupts the ionic gradients and osmotic balance across the apical membrane and eventually causes the epithelial midgut cells to lyse [1].

Several Cry toxins have been shown to form ion-selective channels in artificial receptor-free lipid bilayer membranes at high concentrations (generally above 80 nM): Cry1Aa [2–6], Cry1Ac [4,7–9], Cry1B [4], Cry1C [10,11], Cry2A [12], Cry3A [7] and Cry3Bb [13]. In most cases, multiple conductance levels were observed suggesting that the channels, like those formed by several other bacterial toxins [14], could result from the multimeric assembly of a variable number of toxin molecules [15]. For instance, in symmetrical KCl solutions, Cry1C induces 7–12 conductance levels displaying similar weakly cationic selectivity [10,11]. Multiple conductance levels were also observed when purified receptor proteins [4] or larval

Abbreviations: PEG, polyethylene glycol; POPC, 1-palmitoyl-2-oleoyl-*sn*-glycero-3-phosphatidylcholine; POPE, 1-palmitoyl-2-oleoyl-*sn*-glycero-3-phosphatidylethanolamine

* Corresponding author. Groupe de recherche en transport membranaire, Université de Montréal, P.O. Box 6128, Centre Ville Station, Montreal, Quebec, Canada H3C 3J7. Tel.: +1-514-343-6364; fax: +1-514-343-6631.
E-mail address: jean-louis.schwartz@umontreal.ca (J.-L. Schwartz).

0005-2736/02/$ - see front matter © 2002 Elsevier Science B.V. All rights reserved.
PII: S0005-2736(02)00605-3

midgut brush border membranes [6,16] were incorporated into the lipid bilayer although, under these conditions, some of the toxin channel properties were modified.

The multiple conductance levels could result from the formation of several multimeric pore structures, differing in channel diameter, or from the synchronous gating of several identical channel units forming clusters within the lipid bilayer, as was proposed previously for *B. thuringiensis* toxins [6,7] and demonstrated for various types of ion channels [17–22]. To discriminate between these two possibilities, the size of the pores formed by Cry1C was estimated, in the present study, from the effect of non-electrolyte polymers, polyethylene glycols (PEGs) of various molecular weights ranging from 200 to 10 000, on conductance levels. Non-electrolytes such as PEG have been used to estimate the radius and investigate the lumen geometry of the aqueous pores formed by several bacterial [21,23–30], fungal [18,22,31] and spider venom [17,25] toxins as well as different endogenous cellular channels [32–34] reconstituted in planar lipid bilayers. PEGs behave approximately like spherical molecules in aqueous solutions [35,36] and, at constant w/v concentration, their influence on the bulk solution conductivity is independent of their molecular weight [23]. Single-channel conductance, however, is only reduced when the non-electrolyte molecule is sufficiently small to penetrate into the lumen of the channel, thus allowing channel diameter to be estimated from the hydrated radius of the smallest polyethylene glycol that is excluded from the channel [25]. Using this approach, Cry1C was found to form clusters composed of a variable number of similar channels each having a maximal pore radius of 1.0–1.3 nm. A preliminary account of this work was published earlier in the form of a short conference abstract [37].

2. Materials and methods

2.1. Chemicals and solutions

The phospholipids 1-palmitoyl-2-oleoyl-*sn*-glycero-3-phosphatidylethanolamine (POPE) and 1-palmitoyl-2-oleoyl-*sn*-glycero-3-phosphatidylcholine (POPC) were obtained from Avanti Polar Lipids (Alabaster, AL, USA). All other chemicals were purchased from Sigma-Aldrich (Oakville, Ontario, Canada).

Planar lipid bilayer experiments were conducted under symmetrical conditions with a standard ionic solution composed of 300 mM KCl, 5 mM $CaCl_2$, 0.5 mM EDTA and 5 mM Tris–HCl (pH 8.0). In experiments carried out to determine channel size, 20% (w/v) PEG with molecular weights ranging from 200 to 10 000 was included in this standard solution. Bulk solution conductivities (χ) were measured with a type CDM2e conductimeter and a CDC 104 electrode (Radiometer A/S, Copenhagen, Denmark) (Table 1).

Table 1
PEG hydrodynamic radii and experimental solution conductivities

PEG[a] (M_n)	Hydrodynamic radius (r_h)[b] (nm)	Conductivity (χ)[c] (mS/cm)
None	–	42.8 ± 0.5
200	0.43	23.5 ± 0.5
300	0.60	22.9 ± 0.3
400	0.70	21.1 ± 0.1
600	0.80	22.8 ± 0.4
1000	0.94	22.4 ± 0.9
1500	1.05	21.8 ± 1.1
3400	1.63	22.7 ± 0.3
8000	3.05	21.4 ± 0.1
10 000	3.51[d]	21.7 ± 0.2

[a] Number-average molecular weight values (M_n) were taken from the Aldrich Chemical Company (Milwaukee, WI, USA) catalogue.

[b] Hydrodynamic radii, based on viscometry, are those reported by Krasilnikov et al. [24] and Merzlyak et al. [29].

[c] The standard ionic solution was composed of 300 mM KCl, 5 mM $CaCl_2$, 0.5 mM EDTA and 5 mM Tris–HCl (pH 8.0), with or without 20% (w/v) PEG. Values are means ± S.D. of three determinations.

[d] This value was calculated using the relation between r_h and molecular weight given by Sabirov et al. (Eq. (4) from Ref. [25]).

Recombinant Cry1C toxin was produced as insoluble inclusions in *Escherichia coli*, trypsin activated and purified by fast protein liquid chromatography as described previously [38].

2.2. Planar lipid bilayer experiments

The methods used for planar lipid bilayer experiments and single-channel analysis were described in detail in previous studies [6,39]. Briefly, planar phospholipid bilayer membranes were formed with a 1:1 (w/w) mixture of POPE and POPC at a lipid concentration of 25 mg/ml in 99% *n*-decane. Membranes had a typical capacitance of about 250 pF and could remain stable for several hours. Before toxin incorporation, bilayers were monitored under holding voltage conditions for more than 20 min to ensure that no contaminant-induced activity was present. Trypsin-activated Cry1C was then added to the *trans* chamber at a final concentration of 5–25 μg/ml (77–385 nM). Because spontaneous toxin insertion was quite inefficient, incorporation was promoted mechanically [6,39,40] in some experiments by gently touching the bilayer with a 150-μm-diameter "finger plugger" dental probe (SDS Kerr, Orange, CA, USA) previously dipped in the Cry1C stock solution. When channels failed to appear within 15 min, the bilayer was ruptured and repainted. All experiments were performed at room temperature (22–25 °C).

2.3. Data recording and analysis

Current was measured with Ag/AgCl electrodes connected via agar salt bridges (4% in 1 M KCl) to the *cis* and *trans* solutions bathing the bilayer. Holding voltages were applied to the *cis* chamber relative to the *trans*

chamber, which was grounded. Channel currents were recorded with an Axopatch-1D patch-clamp amplifier (Axon Instruments, Foster City, CA, USA). Currents were filtered at 500 Hz and digitized off-line at 4 KHz. Analysis was performed on a personal computer using a Digidata 1200 series interface and Axotape and pClamp version 6.0 software (Axon Instruments).

For each experiment, several 60–120 s current recordings were obtained at different holding voltages varying from −120 to +120 mV and carefully examined using the Fetchan program (pClamp software version 6.0). The amplitude of a large number of resolvable current steps was measured either by fitting multiple Gaussian curves to all-point histograms of several representative record segments or using cursor measurements when amplitude histograms failed to display peaks corresponding to clearly resolved current levels for rare or brief events. For each applied voltage, current step amplitudes were then averaged over a number of similarly sized steps and plotted against voltage. Conductances (g) were determined as the slopes of the curves obtained by linear regression on the data points. Finally, the corresponding conductance values obtained in different experiments were averaged over the number of experiments in which they were observed.

2.4. Pore size determination

The maximal pore radius of the channels incorporated into bilayer membranes was determined using the procedure described by Krasilnikov et al. [24,32] and Sabirov et al. [25]. Conductances were measured in the different 20% PEG-containing bathing solutions and the ability of these non-electrolytes to penetrate the channels was quantified by calculating the filling parameter (F) [27–30] using the following equation:

$$F = [(G_0 - G_{PEG})/G_{PEG}]/[(\chi_0 - \chi_{PEG})/\chi_{PEG}] \quad (1)$$

where G_0 and G_{PEG} are the conductances measured in 300 mM KCl buffered solutions without and with 20% PEG, respectively, and χ_0 and χ_{PEG} are the electrical conductivities of the corresponding solutions. F reflects the portion of the channel length filled with PEGs. Plotting F against the hydrated radius r_h of the PEGs allows the maximum pore radius (i.e. that of the largest entrance of the pores) to be estimated from the intercept between the decreasing linear part of the relation (where PEG is able to enter into the pore lumen) and the lower quasi-horizontal line (where PEG is excluded from the pore and F is approaching 0).

3. Results

3.1. Cry1C channel activity in the absence of PEG

Representative recordings of Cry1C channel activity, under symmetrical 300 mM KCl, pH 8.0, conditions are illustrated in Fig. 1. Channel activity could vary greatly from one bilayer experiment to another, but recordings were usually characterized by either long periods of closure interrupted by bursts of current jumps (Fig. 1, traces i and vi), rapid flickering (Fig. 1, trace ii), or relatively long

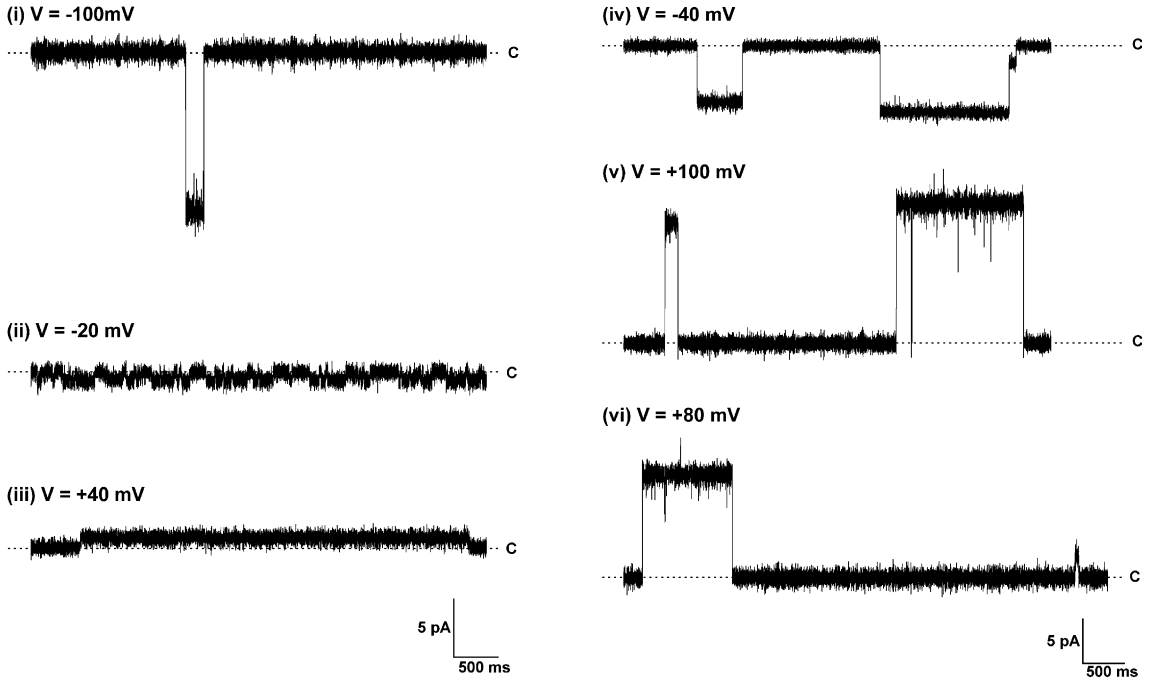

Fig. 1. Channels formed by Cry1C in the absence of PEGs. Representative segments of typical current traces recorded in symmetrical 300 mM KCl solutions at various holding voltages (V). The current levels corresponding to the closed state of the channels (c) are indicated by the dashed lines.

periods in which a single (Fig. 1, traces iii and v) or a small number of openings (Fig. 1, trace iv) were observed. In all bilayer experiments, channel activity involved current steps displaying multiple amplitudes with most steps occurring from the closed state. Large well-defined current steps such as that illustrated in Fig. 1 (trace i) were observed. Because they occurred repeatedly, they did not appear to result from the coincidental superimposition of independent smaller ones. These large current steps were not observed in all experiments.

The number of conductance levels as well as their distribution varied from one experiment to another and during the course of each experiment. Pooling the data collected in seven experiments allowed a total of at least 15 main conductance levels to be identified (Fig. 2). Current–voltage relationships were linear, demonstrating an ohmic behavior, with conductances varying from 21 to 246 pS. The distribution of most conductance levels was characterized by increments of about 10 pS or multiples of 10 pS, suggesting the oligomerization of small channel units. Current steps corresponding to about 10 pS or larger than 300 pS were also occasionally observed, but were not analyzed further because their rare occurrence did not allow current–voltage curves to be constructed.

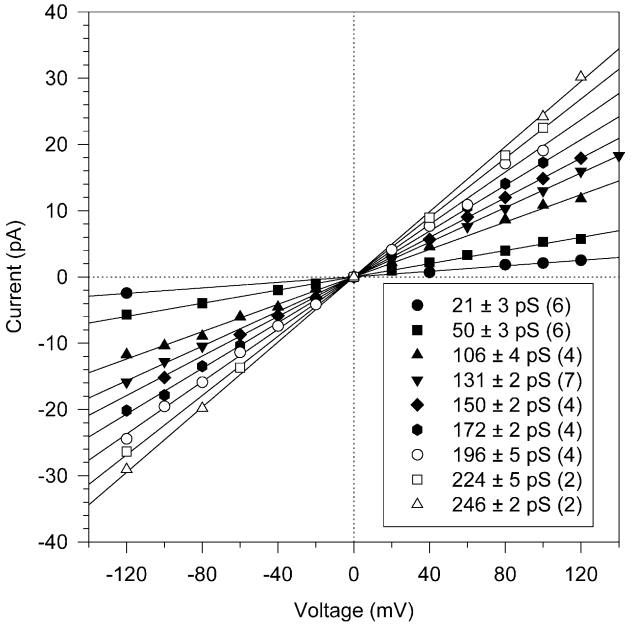

Fig. 2. Current–voltage relationships of the most commonly observed Cry1C current steps. For each experiment and each voltage, current steps were measured and averaged over a number of similar steps. Curves were fitted to the data points by linear regression. Conductances, corresponding to the slopes of the curves, are given as means ± S.D. Results derived from seven experiments were pooled together and the number of experiments in which a given conductance level was detected is shown in parentheses. For clarity, error bars and several current–voltage curves corresponding to conductances of 33 ± 2 pS (n = 5), 41 ± 1 pS (n = 3), 68 ± 3 pS (n = 2), 116 ± 2 pS (n = 2), 140 ± 1 pS (n = 4) and 159 ± 2 pS (n = 5) were omitted.

Table 2
Number and range of main conductance levels observed with or without PEGs

PEG[a] (M_n)	n[b]	N_L[c]	g_{min}[d] (pS)	g_{max}[d] (pS)
None	7	15	21 ± 3 (6)	246 ± 2 (2)
200	5	12	12 ± 1 (3)	162 ± 6 (2)
300	3	14	11 ± 1 (2)	176 ± 1 (2)
400	5	14	13 ± 1 (4)	176 ± 1 (3)
600	5	15	12 ± 1 (4)	174 ± 2 (4)
1000	4	14	12 ± 2 (2)	182 ± 7 (2)
1500	4	13	17 ± 3 (4)	202 (1)
3400	5	15	18 ± 1 (3)	229 ± 5 (2)
8000	3	12	21 ± 3 (3)	219 (1)
10 000	3	15	19 ± 1 (3)	230 ± 5 (2)

[a] Number-average molecular weight values (M_n) were taken from the Aldrich catalogue.
[b] Number of bilayer experiments.
[c] Number of conductance levels identified from current–voltage curves.
[d] Smallest (g_{min}) and largest (g_{max}) conductance levels that could be resolved from current–voltage curves. They were averaged over the number of experiments in which each level was observed (indicated in parentheses). Values are means ± S.D.

3.2. Effect of PEG molecules on Cry1C conductance levels

The presence of PEG molecules in the solutions bathing the bilayer had little influence on its stability and capacitance. Toxin incorporation rates as estimated by channel activity were not appreciably decreased except in the presence of the larger PEGs, probably due to the higher viscosity of the solutions. In the latter case, the toxin dose was increased up to two times. The kinetics of current steps was the same in the presence or in the absence of PEGs. For each PEG-containing solution, conductances were estimated as above from the current–voltage curves. As observed in experiments without PEG, Cry1C displayed multiple ohmic conductance levels and the total number of individual levels observed in different PEG solutions ranged from 12 to 15 (Table 2), independently of the concentration of toxin added to the bath.

The conductances decreased considerably in the presence of the smaller PEGs, indicating that these non-electrolytes readily penetrated into the pore lumen. For example, in the presence of PEG 200, the minimum and maximum conductances were 12 and 162 pS compared to 21 and 246 pS in the absence of PEGs (Table 2). As the size of the PEGs was augmented, the conductances progressively increased until reaching, with PEGs 3400 or larger, values that were comparable to those measured in the absence of PEG, indicating that PEGs larger than or equal to 3400 were completely excluded from the pores.

3.3. Pore size estimated from the smallest (g_{min}) and largest (g_{max}) conductance levels

Most conductance levels differed from one to another by only about 10 pS (Fig. 2), a value which is comparable to the decrease in the smallest conductance due to the presence

of small PEGs (Table 2). Furthermore, the number of conductance levels detected with different PEGs varied. Consequently, pore size could not be unambiguously derived from the conductances estimated from each current–voltage relationship. Therefore, only the smallest (g_{min}) and largest (g_{max}) conductance levels, which were readily identified (Table 2), were considered for analysis.

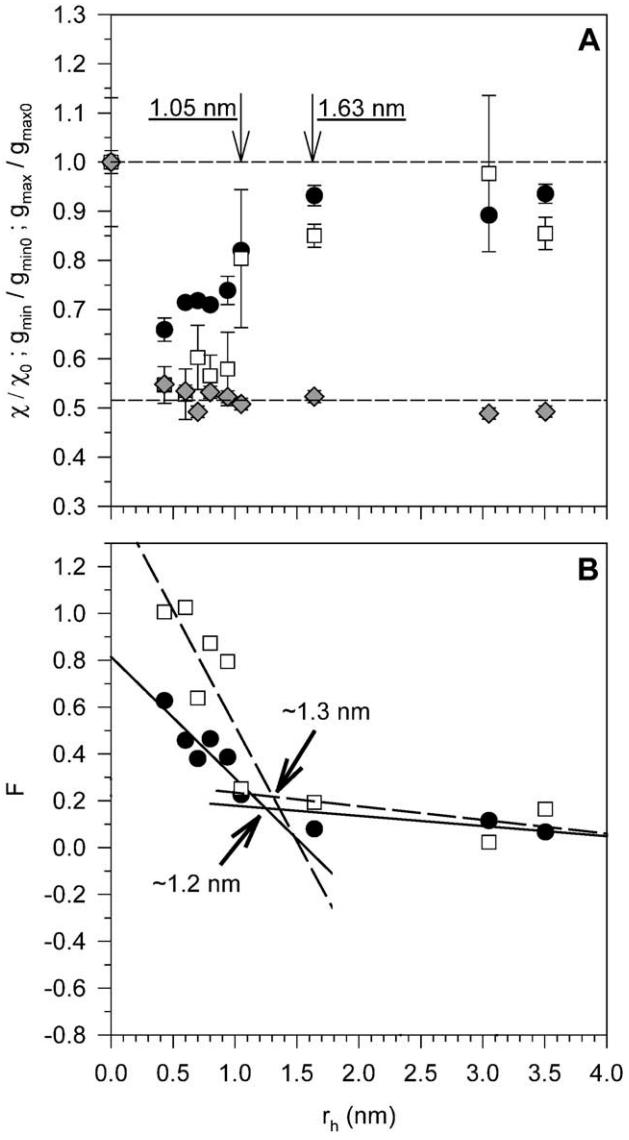

Fig. 3. (A) Effect of PEGs on the bulk solution conductivity χ and the smallest (g_{min}) and largest (g_{max}) conductance levels. For each experimental condition, the conductance was estimated as described in the legend of Fig. 2. The ratios of the conductances measured with and without PEG (g_{min}/g_{min0}, white squares; g_{max}/g_{max0}, black circles) and those of the solution conductivities (χ/χ_0, gray diamonds) calculated under the same conditions were plotted vs. the hydrodynamic radius (r_h) of the PEGs (Table 1). The two dashed lines correspond respectively to the mean ratio of bulk conductivities of the solution with and without PEG (lower line) and to the basal channel conductance measured in the absence of PEG (upper line). Data are means ± S.D. (B) Dependence of the filling parameter (F) on the hydrodynamic radius (r_h) of the PEGs for the smallest (g_{min}, white squares) and largest (g_{max}, black circles) conductances, estimated from current–voltage curves. F was calculated using Eq. (1) described under Materials and methods. Experimental data points obtained for PEG 200 to PEG 1500 and for PEG 1500 to PEG 10000, respectively, for g_{min} (dashed line) and g_{max} (solid line) were fitted by linear regression.

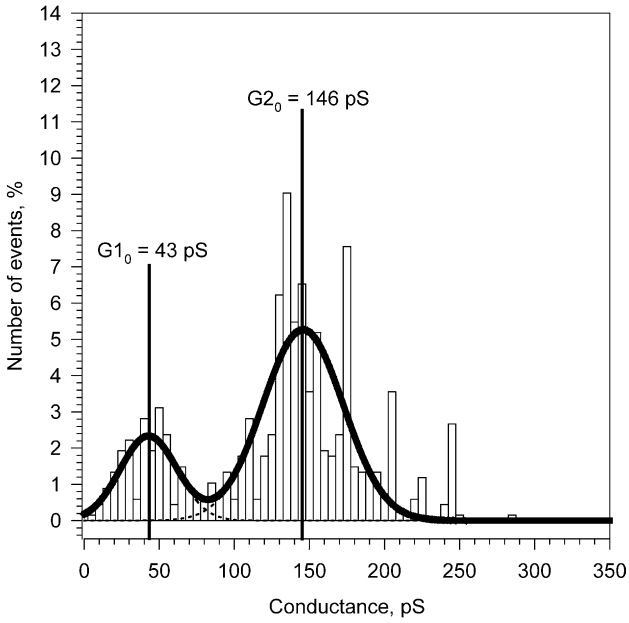

Fig. 4. Frequency distribution of Cry1C conductances observed in the absence of PEGs. Conductances were estimated for each of the 670 current steps observed in the seven experiments and plotted in a cumulative histogram. The bin width is 5 pS. The mean values of the small ($G1_0$) and large ($G2_0$) conductance populations were obtained by fitting a sum of two Gaussian curves (solid line) to the data over the range of 0–350 pS.

To compare the degree to which PEG molecules permeated into the channel pores, the ratio of the conductance measured in the presence and absence of PEGs (g/g_0) was plotted against the hydrodynamic radius of each PEG (Table 1) for both g_{min} and g_{max} conductance values (Fig. 3A). In the presence of PEG 200, channel conductance ratios for both g_{min} and g_{max} were close to that measured for the

Table 3
Mean conductances of Cry1C channels estimated with or without PEGs

PEG[a] (M_n)	n[b]	N[c]	$G1$[d] (pS ± S.E.)	$G2$[d] (pS ± S.E.)	r[e]
None	7	675	43 ± 6	146 ± 3	0.792
200	5	340	30 ± 3	86 ± 8	0.806
300	3	302	34 ± 5	118 ± 2	0.849
400	5	607	29 ± 2	125 ± 2	0.892
600	5	317	36 ± 7	124 ± 1	0.948
1000	4	236	32 ± 5	123 ± 1	0.869
1500	4	398	36 ± 3	141 ± 7	0.728
3400	5	389	44 ± 4	139 ± 7	0.816
8000	3	289	41 ± 4	151 ± 3	0.829
10000	3	243	53 ± 9	155 ± 1	0.894

[a] Number-average molecular weight values (M_n) are taken from the Aldrich catalogue.
[b] Number of bilayer experiments.
[c] Total number of current steps analyzed.
[d] Mean conductance of the small ($G1$) and large ($G2$) conductance populations were obtained by fitting a sum of two Gaussian curves to the data points of the cumulative histograms shown in Figs. 4A and 5.
[e] Correlation coefficient of the Gaussian fit.

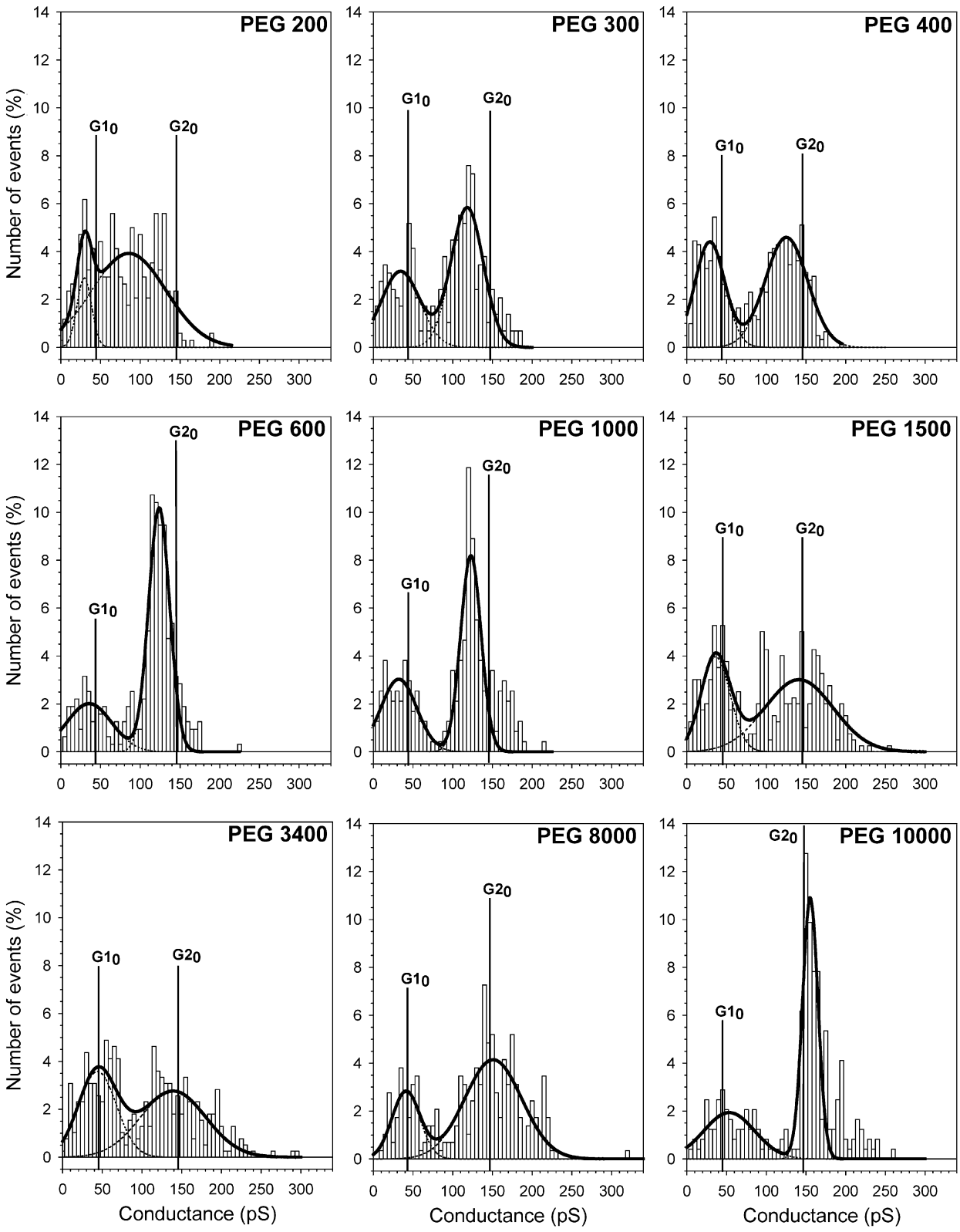

Fig. 5. Effect of PEGs on the distribution of conductances. Experimental conditions were identical to those described in the legend of Fig. 1 except that 20% (w/v) of the indicated PEG was included in the 300 mM KCl solution. For each PEG-containing solution, histograms were constructed from more than 230 current steps recorded in at least three experiments. For comparison, mean conductances obtained for both populations in the absence of PEG are shown by vertical lines.

conductivity of the bulk solution (χ/χ_0), indicating that a PEG of this size penetrated almost freely into the pores. The conductance ratio increased progressively as the radius of the PEG molecules was increased from 0.43 nm (PEG 200) to 1.05 nm (PEG 1500) but reached a value of about 0.9–1.0 (corresponding approximately to that measured without PEG) in the presence of PEGs with a radius of 1.63 nm (PEG 3400) or larger. These results indicate that the radius of the pores corresponding to both the smallest and the largest conductances is in the range of 1.05–1.63 nm.

A more accurate estimate of the pore radius was obtained by plotting the filling parameter (F), calculated with Eq. (1) presented under Materials and methods, against the hydrodynamic radius of the different PEG molecules (Fig. 3B). Data points corresponding to the values obtained for PEGs that were capable of penetrating the pores (PEG 200 to PEG 1500) and for those that were excluded from the pores (PEG 3400 to PEG 10 000) were fitted with two straight lines by linear regression. The maximum radii of the pores formed by Cry1C, given by the abscissa of the intersection point of these curves [27–30], were similar and about 1.2–1.3 nm for both the smallest (g_{min}) and largest (g_{max}) conductances (Fig. 3B).

3.4. Pore size estimated from mean conductance levels

Because unambiguous estimates of pore size could not be obtained for each conductance level identified from current–voltage relationships, another approach, based on the frequency distribution of all recorded current steps, was used to validate the results derived from the g_{min} and g_{max} analysis. The conductance for each step detected in every experiment was calculated by dividing the recorded current by the applied voltage. Since Cry1C conductances are ohmic (Fig. 2), the corresponding values were used to plot frequency distribution histograms. Such a histogram obtained in the absence of PEG is shown in Fig. 4. This cumulative histogram (bin width = 5 pS), constructed from the observation of 670 events, shows two main populations, the largest with most conductances ranging from 100 to about 200 pS (>70% of events) and the smallest corresponding to conductances ranging from 5 to 90 pS. Mean values of 43 ± 6 pS ($G1_0$) and 146 ± 3 pS ($G2_0$) were obtained by fitting a sum of two Gaussian curves to the data over the range of 0 to 350 pS (Table 3).

Cumulative histograms were constructed for each PEG-containing solution (Fig. 5). Similar to those obtained from experiments without PEG, conductances were distributed in two main populations for which the conductances $G1$ and $G2$ were estimated by fitting a sum of two Gaussian curves to the data points (Fig. 5 and Table 3). These values decreased considerably in the presence of the smaller PEGs (Fig. 6A) as was observed previously for g_{min} and g_{max} conductances. For instance, the mean conductances estimated for both populations decreased from 43 pS ($G1_0$) and 146 pS ($G2_0$) without PEG to 30 pS ($G1$) and 86 pS ($G2$) in the presence of PEG 200 (Table 3). As larger PEG molecules were used, the mean conductances increased progressively until reaching, with PEGs 3400 or larger, values that were comparable to $G1_0$ and $G2_0$, indicating that the maximum radius of the pores corresponding to both conductance populations is in the range of 1.05 to 1.63 nm. This result compares well to that obtained from g_{min} and g_{max}.

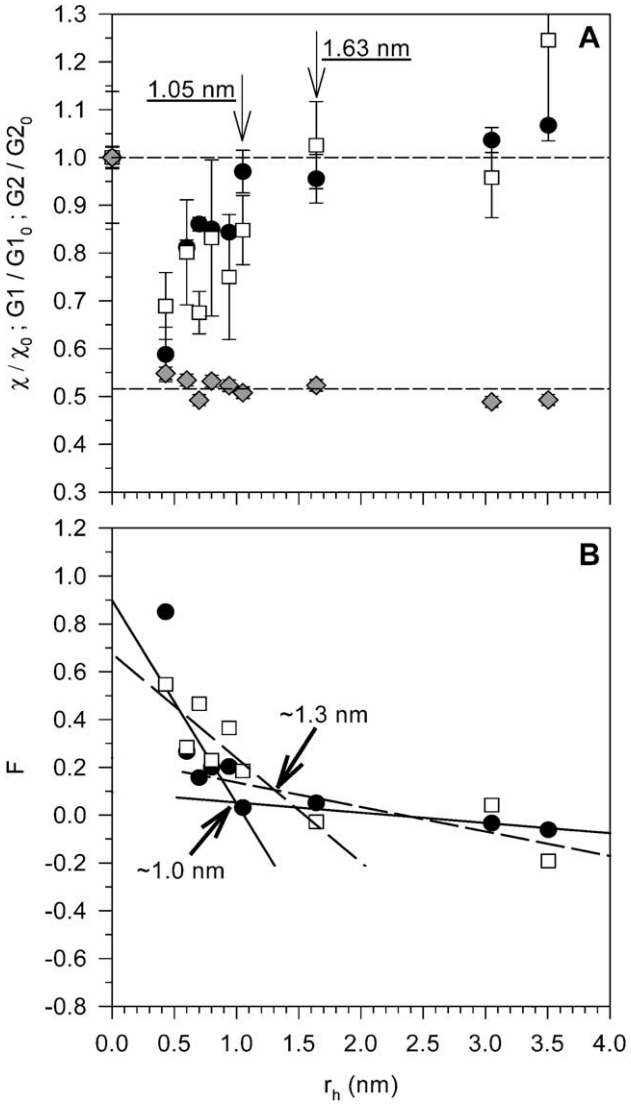

Fig. 6. (A) Effect of PEG on the mean conductance of the Cry1C conductance populations ($G1$ and $G2$). For each bathing solution, the mean conductances were estimated as described in the legend of Fig. 4 and presented as described in the legend of Fig. 3 ($G1/G1_0$, white squares; $G2/G2_0$, black circles). (B) Dependence of the filling parameter (F) on the hydrodynamic radius (r_h) of the PEGs for the small ($G1$, white squares) and large ($G2$, black circles) mean conductances estimated from cumulative histograms (Table 3). F was calculated using Eq. (1) described in Materials and methods. Lines were fitted by linear regression for the small (dashed line) and large (solid line) conductance populations as described in the legend of Fig. 3.

Using the filling parameter procedure described previously, maximal pore radius estimates based on mean con-

ductances $G1$ and $G2$ yielded values of about 1.3 and 1.0 nm (Fig. 6B). Considering the complexity of these analyses and the fact that the size estimated for the smaller mean conductance ($G1$) is larger than of the larger mean conductance ($G2$), these values are probably not different from one another while being in close agreement with those obtained from the analysis of g_{min} and g_{max} values (Fig. 4).

4. Discussion

In this study, the size of the pores formed by Cry1C was estimated using two distinct analytical approaches based on the current–voltage relationships derived from each individual experiment and on the frequency distributions of all recorded conductances, respectively. As pointed out by Hille [41], analysis of complex multichannel recordings, such as those of the present study, is extremely problematic. Limiting pore size estimates to the analysis of the smallest and largest individual conductance levels (g_{min} and g_{max}) or to that of the means of pooled conductance values ($G1$ and $G2$) undoubtedly introduces some degree of simplification. With these procedures, the complexity of Cry1C channel activity could be taken into account, in contrast with most previous studies [4,5,7,10,12,13] in which only the largest or most frequent conductance levels were analyzed in detail. Therefore, subjective interpretations in the analysis were minimized and ambiguities due to the presence of many conductance levels were avoided as much as possible.

This study provides strong evidence that while Cry1C channel activity displays multiple conductance levels, the channels involved have a uniform radius of 1.0–1.3 nm. Multiple conductance levels are therefore probably due to clusters composed of a variable number of similar channels which open and close cooperatively within the membrane. The fact that the number of conductance levels varies from one bilayer to another and during the course of the experiments is also consistent with the occurrence of such clusters within the membrane, allowing for coordinated activity of several channel units [19]. In addition, the frequent observation of complete closures and openings (Fig. 1) occurring as single-current steps also supports the concept of the presence of several independent clusters in the bilayer [20].

Furthermore, cooperative opening of a variable number of channels of similar size is consistent with the fact that all conductance levels identified in the present study were integral multiples of about 10 pS [15]. A similar relation between conductance levels was previously described for the channels formed by Cry1Aa in receptor-free lipid bilayers as well as in bilayers fused with brush border membrane vesicles [6]. Although most previous lipid bilayer studies have focused on the largest or most frequent conductance levels, the existence of intermediate levels was also indicated [4,5,7,9,10,12,13,16]. In addition, it appears from the data presented in some of these studies [9,16] that the larger conductances were integral multiples of the smaller ones. On the other hand, the clusters formed by Cry1C channels tended to distribute in two populations and such a distribution was systematically observed under each of the experimental conditions used in the present study (Figs. 4A and 5). The reason for this behavior is unclear.

The present work provides the first direct evidence of cluster organization of the channels formed by *B. thuringiensis* toxins within membranes. Such functional clusters have been described for the ion channels formed by other pore-forming toxins reconstituted in lipid bilayers, including spider venom α-latrotoxin [17], alamethicin [18], the cyclic lipodepsipeptide syringomycin E [21] and the non-peptidic phytotoxin beticolin 3 [22]. In addition, Larsen et al. [19] have shown, using fluctuation analysis of macroscopic membrane currents and single-channel recordings, that the different levels of conductance displayed by endogenous chloride channels of insect Sf9 cells resulted from the simultaneous gating of a varying number of small but similar channels.

The finding that the pores formed by Cry1C have a uniform size is in agreement with previous reports demonstrating that, in the presence of Cry1Aa [6], Cry1Ac [7], Cry3A [7] and Cry1C [11], similar reversal potentials were estimated for different conductance levels. Similar ion selectivities were also demonstrated from the analysis of different conductance levels induced by Cry1Aa [6] and Cry1C [16] in lipid bilayers into which insect midgut brush border membranes were incorporated. Formation of pores of uniform size is also consistent with our previous kinetic analyses of potassium efflux through the channels formed by Cry1C in Sf9 cells, which yielded a Hill coefficient close to 1 [42].

The pore radius estimated in the present study, in the absence of receptor and proteolytic enzyme, 1.0–1.3 nm, is consistent with data from osmotic swelling experiments [43–46] carried out with insect midgut brush border membrane vesicles. They demonstrated that the pores formed by several *B. thuringiensis* toxins, including Cry1C, allow the diffusion of relatively large molecules such as sucrose (r_h = 0.52 nm [47]) and raffinose (r_h = 0.60 nm [47]) across the membrane. In particular, the present results are in remarkable agreement with previous estimates of 1.2–1.3 nm for the radius of the pores formed by Cry1Ac in brush border membrane vesicles [44].

The pores formed by *B. thuringiensis* toxins are thought to result from the oligomeric assembly of toxin molecules [3,10,48,49]. The results of the present study indicate that such oligomers within the clusters are likely to have a constant stoichiometry, at least under a particular set of experimental conditions. Previous studies have presented evidence that the size of the pores formed by Cry1Ac is influenced by pH [44–46]. Channel radius was estimated to vary from 1.2 nm at pH 8.7 to 1.3 nm at pH 9.8 [44]. These relatively small differences may simply reflect conformational changes affecting the geometry of the channels due to the titration of charged residues within the toxin molecule.

On the other hand, studies have shown that the ion conductance of Cry toxin channels was substantially larger in bilayers into which insect brush-border membranes were incorporated than in receptor-free bilayers [6,16]. Taken together with those of the present study, these results suggest that, in the presence of membrane receptors or other components of the brush border membrane, toxin channels could be organized in clusters composed of a larger number of channel units. It cannot be excluded, however, that, under these conditions, the overall channel architecture could be different. In agreement with this latter possibility, the ion selectivity of the pores formed by Cry1Aa in the presence of brush border membranes was significantly different from that observed in receptor-free bilayers, suggesting an altered charge distribution within the channel lumen [6].

It may appear puzzling that the large pores formed by Cry1C have conductances as low as 10 pS in 300 mM KCl solutions. It is important to note, however, that our estimates were derived from the ability of PEG molecules to penetrate into the channel lumen. Non-electrolyte molecules could influence the conductance of the channel without necessarily diffusing across the whole length of the pore. For this reason, the values presented here correspond to the radius of the widest part of the pore. It remains entirely possible that the lumen of Cry1C channels may be constricted or could have a different radius at each entrance as was reported earlier for colicin Ia [27]. Interestingly, the elementary conductance of Cry1C channels (corresponding to about 10 pS) is in the same range as that of ion channels formed by colicin Ia, which display a conductance of about 90 pS in 1.77 M KCl (corresponding to about 17 pS in our 300 mM KCl conditions) and a radius of about 0.9 nm for the largest pore entrance [27]. Future work should allow to elucidate the detailed structure of the conducting unit, including the fine geometry of its lumen, in the insect midgut membrane environment, and to understand the molecular mechanisms responsible for cluster formation and cooperative gating of *B. thuringiensis* toxin pores.

Acknowledgements

We are grateful to Dr. Jean-François Noulin (Université de Montréal) for stimulating discussions. This work was supported by grants from the Natural Sciences and Engineering Research Council (NSERC) of Canada and the Fonds pour la formation de chercheurs et l'aide à la recherche of Quebec to R. Laprade and J.-L. Schwartz. B. Nieman received a summer student fellowship from NSERC. NRC publication Nr. 45890.

References

[1] E. Schnepf, N. Crickmore, J. Van Rie, D. Lereclus, J. Baum, J. Feitelson, D.R. Zeigler, D.H. Dean, *Bacillus thuringiensis* and its pesticidal crystal proteins, Microbiol. Mol. Biol. Rev. 62 (1998) 775–806.

[2] P. Grochulski, L. Masson, S. Borisova, M. Pusztai-Carey, J.-L. Schwartz, R. Brousseau, M. Cygler, *Bacillus thuringiensis* CryIA(a) insecticidal toxin: crystal structure and channel formation, J. Mol. Biol. 254 (1995) 447–464.

[3] J.-L. Schwartz, M. Juteau, P. Grochulski, M. Cygler, G. Préfontaine, R. Brousseau, L. Masson, Restriction of intramolecular movements within the Cry1Aa toxin molecule of *Bacillus thuringiensis* through disulfide bond engineering, FEBS Lett. 410 (1997) 397–402.

[4] J.-L. Schwartz, Y.-J. Lu, P. Söhnlein, R. Brousseau, R. Laprade, L. Masson, M. Adang, Ion channels formed in planar lipid bilayers by *Bacillus thuringiensis* toxins in the presence of *Manduca sexta* midgut receptors, FEBS Lett. 412 (1997) 270–276.

[5] J.-L. Schwartz, L. Potvin, X.J. Chen, R. Brousseau, R. Laprade, D.H. Dean, Single-site mutations in the conserved alternating-arginine region affect ionic channels formed by CryIAa, a *Bacillus thuringiensis* toxin, Appl. Environ. Microbiol. 63 (1997) 3978–3984.

[6] O. Peyronnet, V. Vachon, J.-L. Schwartz, R. Laprade, Ion channels induced in planar lipid bilayers by the *Bacillus thuringiensis* toxin Cry1Aa in the presence of gypsy moth (*Lymantria dispar*) brush border membrane, J. Membr. Biol. 184 (2001) 45–54.

[7] S.L. Slatin, C.K. Abrams, L. English, Delta-endotoxins form cation-selective channels in planar lipid bilayers, Biochem. Biophys. Res. Commun. 169 (1990) 765–772.

[8] D. Smedley, G. Armstrong, D.J. Ellar, Channel activity caused by a *Bacillus thuringiensis* δ-endotoxin preparation depends on the method of activation, Mol. Membr. Biol. 14 (1997) 13–18.

[9] A. Chandra, P. Ghosh, A.D. Mandaokar, A.K. Bera, R.P. Sharma, S. Das, P.A. Kumar, Amino acid substitution in α-helix 7 of Cry1Ac δ-endotoxin of *Bacillus thuringiensis* leads to enhanced toxicity to *Helicoverpa armigera* Hubner, FEBS Lett. 458 (1999) 175–179.

[10] J.-L. Schwartz, L. Garneau, D. Savaria, L. Masson, R. Brousseau, E. Rousseau, Lepidopteran-specific crystal toxins from *Bacillus thuringiensis* form cation- and anion-selective channels in planar lipid bilayers, J. Membr. Biol. 132 (1993) 53–62.

[11] J. Racapé, D. Granger, J.-F. Noulin, V. Vachon, C. Rang, R. Frutos, J.-L. Schwartz, R. Laprade, Properties of the pores formed by parental and chimeric *Bacillus thuringiensis* insecticidal toxins in planar lipid bilayer membranes, Biophys. J. 72 (1997) A82.

[12] L. English, H.L. Robbins, M.A. Von Tersch, C.A. Kulesza, D. Ave, D. Coyle, C.S. Jany, S.L. Slatin, Mode of action of CryIIA: a *Bacillus thuringiensis* delta-endotoxin, Insect Biochem. Mol. Biol. 24 (1994) 1025–1035.

[13] M.A. Von Tersch, S.L. Slatin, C.A. Kulesza, L.H. English, Membrane-permeabilizing activities of *Bacillus thuringiensis* coleopteran-active toxin CryIIIB2 and CryIIIB2 domain I peptide, Appl. Environ. Microbiol. 60 (1994) 3711–3717.

[14] C. Lesieur, B. Vécsey-Semjéen, L. Abrami, M. Fivaz, F.G. van der Goot, Membrane insertion: the strategies of toxins, Mol. Membr. Biol. 14 (1997) 45–64.

[15] J.A. Fox, Ion channel subconductance states, J. Membr. Biol. 97 (1987) 1–8.

[16] A. Lorence, A. Darszon, C. Díaz, A. Liévano, R. Quintero, A. Bravo, δ-Endotoxins induce cation channels in *Spodoptera frugiperda* brush border membranes in suspension and in planar lipid bilayers, FEBS Lett. 360 (1995) 217–222.

[17] O.V. Krasilnikov, R.Z. Sabirov, Comparative analysis of latrotoxin channels of different conductance in planar lipid bilayers. Evidence for cluster organization, Biochim. Biophys. Acta 1112 (1992) 124–128.

[18] S.M. Bezrukov, I. Vodyanoy, Probing alamethicin channels with water-soluble polymers. Effect on conductance of channel states, Biophys. J. 64 (1993) 16–25.

[19] E.H. Larsen, S.E. Gabriel, M.J. Stutts, J. Fullton, E.M. Price, R.C. Boucher, Endogenous chloride channels of insect Sf9 cells. Evidence for coordinated activity of small elementary channel units, J. Gen. Physiol. 107 (1996) 695–714.

[20] C. Grosman, M.I. Mariano, J.P. Bozzini, I.L. Reisin, Properties of two

multisubstate Cl^- channels from human syncytiotrophoblast reconstituted on planar lipid bilayers, J. Membr. Biol. 157 (1997) 83–95.
[21] Y.A. Kaulin, L.V. Schagina, S.M. Bezrukov, V.V. Malev, A.M. Feigin, J.Y. Takemoto, J.H. Teeter, J.G. Brand, Cluster organization of ion channels formed by the antibiotic syringomycin E in bilayer lipid membranes, Biophys. J. 74 (1998) 2918–2925.
[22] C. Goudet, J.-P. Benitah, M.-L. Milat, H. Sentenac, J.-B. Thibaud, Cluster organization and pore structure of ion channels formed by beticolin 3, a nonpeptidic fungal toxin, Biophys. J. 77 (1999) 3052–3059.
[23] O.V. Krasilnikov, J.N. Muratkhodjaev, S.E. Voronov, Y.V. Yezepchuk, The ionic channels formed by cholera toxin in planar bilayer lipid membranes are entirely attributable to its B-subunit, Biochim. Biophys. Acta 1067 (1991) 166–170.
[24] O.V. Krasilnikov, R.Z. Sabirov, V.I. Ternovsky, P.G. Merzliak, J.N. Muratkhodjaev, A simple method for the determination of the pore radius of ion channels in planar lipid bilayer membranes, FEMS Microbiol. Immunol. 105 (1992) 93–100.
[25] R.Z. Sabirov, O.V. Krasilinikov, V.I. Ternovsky, P.G. Merzliak, Relation between ionic channel conductance and conductivity of media containing different nonelectrolytes. A novel method of pore size determination, Gen. Physiol. Biophys. 12 (1993) 95–111.
[26] Y.E. Korchev, C.L. Bashford, G.M. Alder, J.J. Kasianowicz, C.A. Pasternak, Low conductance states of a single ion channel are not 'closed', J. Membr. Biol. 147 (1995) 233–239.
[27] O.V. Krasilnikov, J.B. Da Cruz, L.N. Yuldasheva, W.A. Varanda, R.A. Nogueira, A novel approach to study the geometry of the water lumen of ion channels: colicin Ia channels in planar lipid bilayers, J. Membr. Biol. 161 (1998) 83–92.
[28] O.V. Krasilnikov, P.G. Merzlyak, L.N. Yuldasheva, R.A. Nogueira, Channel-sizing experiments in multichannel bilayers, Gen. Physiol. Biophys. 17 (1998) 349–363.
[29] P.G. Merzlyak, L.N. Yuldasheva, C.G. Rodrigues, C.M.M. Carneiro, O.V. Krasilnikov, S.M. Bezrukov, Polymeric nonelectrolytes to probe pore geometry: application to the α-toxin transmembrane channel, Biophys. J. 77 (1999) 3023–3033.
[30] L.N. Yuldasheva, P.G. Merzlyak, A.O. Zitzer, C.G. Rodrigues, S. Bhakdi, O.V. Krasilnikov, Lumen geometry of ion channels formed by *Vibrio cholerae* EL Tor cytolysin elucidated by nonelectrolyte exclusion, Biochim. Biophys. Acta 1512 (2001) 53–63.
[31] G. Tadjibaeva, R. Sabirov, T. Tomita, Flammutoxin, a cytolysin from the edible mushroom *Flammulina velutipes*, forms two different types of voltage-gated channels in lipid bilayer membranes, Biochim. Biophys. Acta 1467 (2000) 431–443.
[32] O.V. Krasilnikov, C.M.M. Carneiro, L.N. Yuldasheva, A.C. Campos-de-Carvalho, R.A. Nogueira, Diameter of the mammalian porin channel in open and "closed" states: direct measurement at the single channel level in planar lipid bilayer, Braz. J. Med. Biol. Res. 29 (1996) 1691–1697.
[33] C.M.M. Carneiro, O.V. Krasilnikov, L.N. Yuldasheva, A.C. Campos de Carvalho, R.A. Nogueira, Is the mammalian porin channel, VDAC, a perfect cylinder in the high conductance state? FEBS Lett. 416 (1997) 187–189.
[34] S.A. Desai, R.L. Rosenberg, Pore size of the malaria parasite's nutrient channel, Proc. Natl. Acad. Sci. U. S. A. 94 (1997) 2045–2049.
[35] P. Rempp, Contribution à l'étude des solutions de molécules en chaînes à squelette oxygéné, J. Chim. Phys. 54 (1957) 421–467.
[36] R. Scherrer, P. Gerhardt, Molecular sieving by the *Bacillus megaterium* cell wall and protoplast, J. Bacteriol. 107 (1971) 718–735.
[37] O. Peyronnet, F. Généreux, B. Nieman, V. Vachon, R. Laprade, J.-L. Schwartz, Pore size of ion channels formed by the *Bacillus thuringiensis* Cry1C toxin, Med. Microbiol. Immunol. 189 (2000) 44.
[38] L. Masson, G. Préfontaine, L. Péloquin, P.C.K. Lau, R. Brousseau, Comparative analysis of the individual protoxin components in P1 crystals of *Bacillus thuringiensis* subsp. *kurstaki* isolates NRD-12 and HD-1, Biochem. J. 269 (1989) 507–512.
[39] O. Peyronnet, V. Vachon, J.-L. Schwartz, R. Laprade, Ion channel activity from the midgut brush-border membrane of gypsy moth (*Lymantria dispar*) larvae, J. Exp. Biol. 203 (2000) 1835–1844.
[40] N. Denicourt, S. Cai, L. Garneau, M.G. Brunette, R. Sauvé, Evidence from incorporation experiments for an anionic channel of small conductance at the apical membrane of the rabbit distal tubule, Biochim. Biophys. Acta 1285 (1996) 155–166.
[41] B. Hille, Ionic Channels of Excitable Membranes, Sinauer Associates, Sunderland, MA, 1992, pp. 326–328.
[42] G. Guihard, V. Vachon, R. Laprade, J.-L. Schwartz, Kinetic properties of the channels formed by the *Bacillus thuringiensis* insecticidal crystal protein Cry1C in the plasma membrane of Sf9 cells, J. Membr. Biol. 175 (2000) 115–122.
[43] J. Carroll, D.J. Ellar, An analysis of *Bacillus thuringiensis* δ-endotoxin action on insect-midgut-membrane permeability using a light-scattering assay, Eur. J. Biochem. 214 (1993) 771–778.
[44] J. Carroll, D.J. Ellar, Analysis of the large aqueous pores produced by a *Bacillus thuringiensis* protein insecticide in *Manduca sexta* midgut-brush-border-membrane vesicles, Eur. J. Biochem. 245 (1997) 797–804.
[45] F. Coux, V. Vachon, C. Rang, K. Moozar, L. Masson, M. Royer, M. Bes, S. Rivest, R. Brousseau, J.-L. Schwartz, R. Laprade, R. Frutos, Role of interdomain salt bridges in the pore-forming ability of the *Bacillus thuringiensis* toxins Cry1Aa and Cry1Ac, J. Biol. Chem. 276 (2001) 35546–35551.
[46] L.B. Tran, V. Vachon, J.-L. Schwartz, R. Laprade, Differential effects of pH on the pore-forming properties of *Bacillus thuringiensis* insecticidal crystal toxins, Appl. Environ. Microbiol. 67 (2001) 4488–4494.
[47] S.G. Schultz, A.K. Solomon, Determination of the effective hydrodynamic radii of small molecules by viscometry, J. Gen. Physiol. 44 (1961) 1189–1199.
[48] A.I. Aronson, C. Geng, L. Wu, Aggregation of *Bacillus thuringiensis* Cry1A toxins upon binding to target insect larval midgut vesicles, Appl. Environ. Microbiol. 65 (1999) 2503–2507.
[49] M. Soberón, R.V. Pérez, M.E. Nuñez-Valdéz, A. Lorence, I. Gómez, J. Sánchez, A. Bravo, Evidence for intermolecular interaction as a necessary step for pore-formation activity and toxicity of *Bacillus thuringiensis* Cry1Ab toxin, FEMS Microbiol. Lett. 191 (2000) 221–225.